In vivo determination of electric conductivity and permittivity using "Electric Properties Tomography" (EPT)

U. Katscher[1], T. Dorniok[2], C. Findeklee[1], and P. Vernickel[1]

[1]Philips Research Laboratories, Hamburg, Germany, [2]Free University of Berlin, Berlin, Germany

Introduction: The electric properties of human tissue, i.e., the electric conductivity σ and permittivity ε, can potentially be used as an additional diagnostic parameter or might be helpful for a more precise prediction of the local SAR distribution during MR measurements [1]. Recently, a new approach "Electric Properties Tomography" (EPT) was presented, which derives the patient's electric properties from the spatial sensitivity distributions of the applied Tx/Rx RF coil of a standard MR system [2]. In contrast to previous methods to measure the patient's electric properties [3-5], EPT does not apply externally mounted electrodes or currents, thus enhancing the practicability of the approach. Moreover, in opposite to the previous methods, EPT might circumvent the solution of an inverse problem, which could lead to significantly higher spatial image resolution. In this study, first in vivo measurements of healthy volunteers are presented. In the legs, differences in the measured σ and ε of fat, muscle, and bone marrow can be distinguished. In brain measurements of σ and ε, the cerebro-spinal fluid (CSF) of the ventricles can be delineated from the surrounding white matter.

Theory: From Maxwell's equations, we obtain

$$\nabla \times \underline{\vec{H}}(\vec{r}) = i\omega \underline{\varepsilon}(\vec{r}) \underline{\vec{E}}(\underline{\varepsilon}(\vec{r}), \vec{r}) \qquad (1)$$

with $\underline{H}$ the magnetic field strength, $\underline{E}$ the electric field, ω the Larmor frequency, and $\underline{\varepsilon}$ the (supposed to be isotropic) permittivity. The underlinings denote complex variables. Eq. (1) can be solved for the unknown $\underline{\varepsilon}$ by regarding only the z-component

$$\left(\partial_x \underline{H}_y(\vec{r}) - \partial_y \underline{H}_x(\vec{r})\right) \Big/ \underline{E}_z(\underline{\varepsilon}(\vec{r}), \vec{r}) = i\omega \underline{\varepsilon}(\vec{r}) \cdot \qquad (2)$$

The real and imaginary part of $\underline{\varepsilon}$ can be identified with the (non-complex) permittivity ε and the electric conductivity σ, respectively. $\underline{H}_x$ and $\underline{H}_y$ can be measured via MRI by utilizing the sensitivities $\underline{H}^+$ and $\underline{H}^-$ of an RF coil for the transmit and receive case, respectively. For instance, $\underline{H}^+$ and $\underline{H}^-$ can be determined by fitting a sinus in each pixel of a series of flip angles α_n ($\underline{S}_n$ the images for the different flip angles, *const* a system-dependent constant) [6]

$$\underline{S}_n(\alpha_n, \vec{r}) \sim \underline{H}^-(\vec{r}) \sin(const \cdot \alpha_n \cdot \underline{H}^+(\vec{r})) \cdot \qquad (3)$$

These sensitivities are given by the $\underline{H}$ component circularly polarized in the positive and negative direction, respectively

$$\underline{H}^+ = \left(\underline{H}_x + i\underline{H}_y\right)/2 \;\; , \;\; \underline{H}^- = \left(\underline{H}_x - i\underline{H}_y\right)/2 \cdot \qquad (4)$$

Thus, the wanted components $\underline{H}_x$ and $\underline{H}_y$ can be deduced from Eq. (4). Finally, $\underline{E}_z$ has to be estimated via simulations in order to solve Eq. (2). The corresponding simulation setup is given by the (known) RF coil geometry and the patient's geometry known from the measurement of $\underline{H}^+$ and $\underline{H}^-$. Furthermore, since E_z itself is a function of $\underline{\varepsilon}$, an iteration has to be applied

$$\left(\partial_x \underline{H}_y(\vec{r}) - \partial_y \underline{H}_x(\vec{r})\right) \Big/ \underline{E}_z(\underline{\varepsilon}^n(\vec{r}), \vec{r}) = i\omega \underline{\varepsilon}^{n+1}(\vec{r}) \cdot \qquad (5)$$

The iteration starts with an estimation $\underline{\varepsilon}^0$, e.g., literature values of healthy tissue (see, e.g., [1]). However, simulations showed, that even without iteration, i.e., using E belonging to $\underline{\varepsilon}^0$, a diagnostically useful, "$\underline{\varepsilon}$ - weighted" image is achieved [2].

Methods: Legs and head of a healthy volunteer have been investigated. The legs contain three major compartments differing in $\underline{\varepsilon}$ (muscle: ε_r=71.73, σ=0.74 S/m, fat: ε_r=13.64, σ=0.07 S/m, bone marrow: ε_r=16.43, σ=0.15 S/m) [1]. For the brain, the aim was to distinguish between CSF in the ventricles (ε_r=97.31, σ=2.07 S/m) and the surrounding white matter (ε_r=67.84, σ=0.29 S/m) [1]. The electric fields have been simulated using the software package CONCEPT II [7]. The legs were modeled by cones, and the head was modeled by an ellipsoid. Transverse TSE images were acquired on a standard Philips Achieva 1.5T system. For the legs, the Tx/Rx body coil was used (TE/TR = 12/3000ms, resolution 3.5×3.5×10mm). For the brain, a Tx/Rx birdcage head coil was applied (TE/TR = 12/3000ms, resolution 2×2×10mm). For both experiments, eight different flip angles α=10°,30°,…,130°,150° were applied and $\underline{H}^+$ of the two coils fitted via Eq. (3) using a Levenberg-Marquardt algorithm [8]. The quadrature nature of the coils leads to $\underline{H}^+ >> \underline{H}^-$. For this reason, standard MR systems switch the coil polarization between transmit and receive phase, and thus, $\underline{H}^-$ cannot be derived from Eq. (3). Two different work-arounds for this problem have been tested: (A) Due to $\underline{H}^+ >> \underline{H}^-$, $\underline{H}^- = 0$ is assumed. (B) Not only $\underline{E}$ is taken from the simulation, but also $\underline{H}^-$, and is iterated in the same way as $\underline{E}$ via Eq. (5).

Results: Figure 1 shows the reconstructed σ and ε of the leg. The lower halfs of Fig. 1 show the "raw" images for $\alpha = 90°$. The iteration (5) started with assigning the literature values for muscle for all three compartments, i.e., an electrically homogeneous model. After 5 iterations, the bone marrow as well as the fat rim shows clearly reduced values of σ and ε_r (Fig 1). In this example, $\underline{H}^-$ has been iterated and taken from the simulation in analogy to the electric field. Figure 2 shows the "raw" image (right) and the reconstructed ε_r (left) of the head. Here, only one ellipsoid compartment for the whole head has been used, and thus, no iteration has been applied. In this example, $\underline{H}^-$ has been neglected due to $\underline{H}^+ >> \underline{H}^-$. Differences in CSF in the ventricles and the surrounding white matter are visible.

Discussion/Conclusion: A method is presented determining the electric conductivity and permittivity of human tissue, based on the determination of the spatial sensitivity distributions of the involved RF coils. The corresponding electric fields of the RF coils have to be determined numerically. First in vivo experiments have been performed with a standard MR system. The satisfying results might serve as an initial proof of principal for the approach. Neglecting the time-consuming iteration might be sufficient, if only "$\underline{\varepsilon}$-weighted" images are required. Using the iteration, absolute values of $\underline{\varepsilon}$ might be obtained. In the near future, the measurement of $\underline{H}^-$ should be facilitated by multi-element transmit systems, offering direct control of the polarization direction of the Tx/Rx fields.

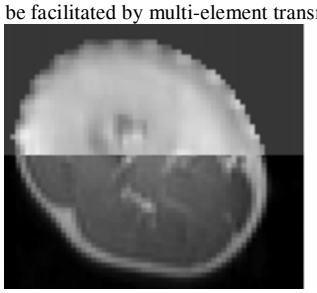

Fig. 1(a)

Fig. 1(b)

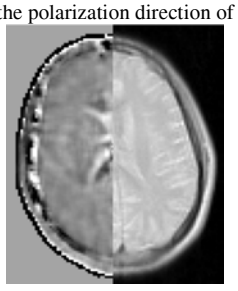

Fig. 2

Fig. 1: Lower half: raw MR image of the right leg for α=90°. Upper half: corresponding reconstructed (a) conductivity and (b) permittivity. Differences between the muscle, the central bone marrow, and the fat rim can be distinguished. Fig. 2: Right half: raw MR image of the head for α=90°. Left half: corresponding reconstructed permittivity. Differences in CSF in the ventricles (central X-shaped compartment) and the surrounding white matter are visible.

References: [1] Joines WT et al. *Med. Phys.* 21 (1994) 54 [2] Katscher U et al. *Proc. ISMRM* 14 (2006) 3035,3037 [3] Saulnier GJ et al. *IEEE Sig. Proc. Mag.* 18 (2001) S31 [4] Gencer NG et al. *IEEE Trans on Biomed. Eng.* 43 (1996) 139 [5] Huang F et al. *Proc. ISMRM* 13 (2005) 683, [6] Collins CM et al. *MRM* 47 (2002) 1026 [7] CONCEPT II, Technical University Hamburg–Harburg, Department of Theoretical Electrical Engineering [8] Press WH et al. *Numerical Recipies in C*. Cambridge University Press, 1995